Korean J. Chem. Eng., **27**(4), 1301-1309 (2010)
DOI: 10.1007/s11814-010-0173-z

Influence of aging conditions on textural properties of water-glass-based silica aerogels prepared at ambient pressure

Pradip Bhikaji Sarawade, Jong-Kil Kim, Askwar Hilonga, and Hee Taik Kim†

Department of Chemical Engineering, Hanyang University 2-260, Ansan, Gyeonggi-do 426-791, Korea
(*Received 17 July 2009 • accepted 4 November 2009*)

Abstract−The experimental results of aging time and temperature on the textural properties of water-glass (sodium silicate)-based silica aerogels are reported and discussed. Aging of the hydrogel for different times and temperatures led to an ability to increase the stiffness and strength of the networks. These improvements enabled the gel to withstand ambient pressure drying (APD) and, consequently, preserve the highly porous silica network without collapse. The pore size and volume increased with increasing aging temperature and time, while the specific surface area decreased. Monolithic aerogels with extremely low bulk density (~0.069 g/cm^3), high specific surface area (820 m^{2}g^{-1}), large cumulative pore volume (3.8 cm^{3}g^{-1}), and high porosity (~96%) were obtained by aging at 60 °C for 18 hours. Therefore, easy synthesis of monolithic silica aerogels at ambient pressure is achievable using a relatively inexpensive silica precursor (sodium silicate).

Key words: Silica Aerogels, Sodium Silicate, Ambient Pressure, Monolithic

INTRODUCTION

Silica aerogels are light, man-made ultra-nanoporous solid materials with large surface area (~1,100 m^2/g), high porosity (80-98%), low bulk density (~0.03 g/cm^3), extremely low thermal conductivities (0.005 W/mk), and fascinating acoustic properties (sound velocities as low as 100 m/s) [1,2]. As a result, aerogels have a variety of potential applications, such as thermal super-insulators in solar energy systems, refrigerators, thermos flasks [3], internal confinement fusion (ICF) targets for thermonuclear fusion reactions [4], very efficient catalysts and catalytic supports [5,6], storage media for liquids in rocket propellants [7], and radio luminescent devices [8]. Additionally, monolithic silica aerogels have been used extensively in high-energy physics in Cherenkov radiation detectors [9,10]. The extremely low densities and high surface areas of monolithic aerogels allow improving the performance of various metal-oxide-based devices, including gas and biosensors, batteries, heterogeneous catalysis devices, space launch applications, and dielectric constant materials for integrated circuits (low-k dielectrics) [11-14].

Conventionally, silica aerogels are prepared via sol-gel polymerization of high-cost hazardous alkoxides [TMOS or TEOS] through supercritical drying, by removing the entrapped solvent from the wet gel while maintaining the integrity and high porosity of the gel [15]. However, supercritical drying has limitations in terms of cost and safety, as it involves heating and evacuation of flammable solvents at high temperature (260 °C) and pressure (~100 bars). As a result, a method to produce silica aerogels using low-cost inorganic precursors, such as sodium silicate (water-glass), at low temperature and pressure is needed. Ambient pressure drying (APD) is competitive in terms of cost and safety, and the preparation of silica aerogels has been extensively studied over many years [16-20]. Nevertheless, the synthesis of monolithic silica aerogels using sodium silicate at an ambient pressure is scarcely reported. Optimization of aging conditions and modification processes are of prime importance for the synthesis of monolithic silica aerogels (without cracks) at an ambient pressure. In this process, the gel undergoes a "spring-back effect" during the drying and preserves porosity and prevents cracks in the dried solid [21,22]. Otherwise, the gel shrinks to accommodate the loss of pore fluid, producing severe cracks in the aerogels during APD. Therefore, many efforts have been made to increase the strength of silica aerogels (before drying) to obtain low density-monolithic silica aerogels at an ambient pressure [23,24]. Gel aging is a key factor in strengthening the gel network and enhancing the backbone strength to prevent the collapse or cracking of silica aerogels during APD [25,26]. The aging conditions have a strong impact on the textural and physical properties of the silica aerogel [27]. Although Zhao et al. [28] recently reported the modified aging process for TEOS-based silica aerogels, there are few reports on the effect of preparation and aging conditions on the pore structure of silica gels derived from alkoxides (TMOS or TEOS) and water-glass [29-32]. Moreover, to the best of our knowledge, there are no reports on the combined effect of aging time and temperature on the physicochemical properties of sodium silicate-based silica aerogels.

In the present study, we concisely report the combined effect of aging time and temperature on the textural and physicochemical properties of sodium silicate-based silica aerogels (dried at ambient pressure). Simultaneous solvent exchange and surface modification processes were employed to reduce the synthesis duration of monolithic aerogels from 7 to ~3 days. Moreover, the effect of the aging conditions on the monolithicity of sodium silicate-based silica aerogel synthesized at an ambient pressure was investigated. We have successfully synthesized monolithic aerogels with more desirable density, surface area, and pore volume, using a cheap silica precursor (sodium silicate), at optimized aging conditions.

†To whom correspondence should be addressed.
E-mail: khtaik@hanyang.ac.kr

MATERIALS AND METHODS

1. Preparation of Silica Hydrogels Using Sodium Silicate (Water-glass)

Silica hydrogels were prepared through hydrolysis and polycondensation of sodium silicate as a precursor solution with 24% silica content (molar ratio $SiO_2 : Na_2O=3.24$) (Shinwoo Materials Co. Ltd., South Korea). The silylating agent was trimethylchlorosilane (TMCS) from Duksan Chemical Co. Ltd., South Korea. Initially, the 24 wt% water-glass solution was diluted to 8 wt% with distilled water. Furthermore, for the replacement of Na^+ with H^+, the solution was mixed at a 1 : 1 volume proportion with an ion exchange resin (IR-120, pH 2.4, Fluka Chemicals, Switzerland) and stirred for 30 minutes. The colloidal silica solution was separated by filtration. The initial sodium silicate solution had a pH of about 12, which was reduced to pH 2.4 after stirring with Amberlight. The hydrogel was prepared by gradual addition of a 1 M NH_4OH solution to the colloidal silica solution, resulting in an increase in pH from 2.4 to 6. The as-prepared silica solutions were poured into a 50 ml beaker, made air-tight, and incubated at room temperature for gelation. Thereafter, samples were aged at different conditions of time and temperature.

2. Simultaneous Solvent Exchange/Surface Modification and Drying of the Hydrogel

To minimize the drying shrinkage, the surface of the gels was modified using a methanol/TMCS/n-hexane solution via a one-step solvent exchange surface modification process before APD. The simultaneous solvent exchange and surface modification was performed by immersing the aged hydrogel in a methanol/TMCS/n-hexane at room temperature for 24 hours. To determine the optimum conditions for the one-step surface modification process, the molar ratio of methanol/TMCS (M) was varied from 0.5 to 2. Additionally, the volumetric ratio of hexane and TMCS (V) was varied from 10 to 30. There was no significant effect of the methanol/TMCS molar ratio on the monolithicity of the dried aerogels in the selected range of ratios. Thus, the molar ratio of methanol/TMCS was fixed at one for additional experiments. The volumetric ratio of n-hexane/TMCS was also fixed at 25 since fewer cracks were observed at this ratio and also as reported elsewhere [33]. After the surface modification, the gels were washed with n-hexane to remove the unreacted TMCS. The wet gels were dried at room temperature (~25 °C) for 24 hours and then at 80 °C for two hours to reduce drying shrinkage. For a complete evaporation of the pore liquid, the gels were dried at 200 °C for an hour. The aerogel samples were allowed to cool to room temperature and were characterized by various techniques.

3. Characterization Methods

The bulk densities of the obtained silica aerogels were calculated from their mass to volume ratios. The volume was calculated after the dimensions of the monolithic aerogel were measured by using vernier calipers. An electronic microbalance (Model OHAUS EPG214C USA) was used to measure the mass of the samples. The percent volume shrinkage and porosity of the prepared aerogels were determined, as follows:

$$\% \text{ Volume shrinkage}=(1-V_a/V_g)\times 100 \quad (1)$$

$$\% \text{ Porosity}=(1-\rho_b/\rho_s)\times 100 \quad (2)$$

where, V_a and V_g are the volumes of the aerogel and hydrogel, respectively. ρ_s and ρ_b are the skeletal and bulk densities (of the silica aerogel), respectively.

The specific surface area of the aerogels were analyzed by the Brunauer Emmet and Teller (BET) method, while the pore size distributions (PSDs) were determined by the BJH method (ASAP 2000, Micromeritics, USA). BET analysis from the amount of N_2 gas adsorbed at various partial pressures (ten points $0.05<p/p_o<0.3$, nitrogen molecular cross sectional area=0.162 nm^2) was used to determine the surface area, and a single condensation point ($p/p_o=0.99$) was used to determine the pore volume. Before N_2 adsorption, the sample was degassed at 200 °C. Pore size distributions were calculated from the desorption isotherms [34-36]. To study the thermal stability of the aerogels (in terms of retention of hydrophobicity), the samples were examined by thermogravimetric and differential thermal analysis (TG-DTA). Ten mg of the hydrophobic nanoporous silica aerogels was heat-treated in air from room temperature (25 °C) to 1,000 °C with a controlled heating rate of 1.5 °C min^{-1} using a microprocessor-based Parr temperature controller (Model 4846, USA) connected to a muffle furnace (A. H. JEON Industrial Co. Ltd., Korea). In this study, the thermal stability refers to the temperature up to which the silica aerogel retains its hydrophobicity [37].

The surface modification was confirmed by infrared (IR) spectroscopy, Perkin-Elmer (Model No. 783, USA). For this purpose, the as-prepared monolithic silica aerogels were ground into powders, mixed with KBr, and pressed to form a sample pellet for FTIR measurements. The contact angle (θ) measurements were performed with a contact angle meter (CAM 200 Automates Contact Angle Analyzer, Finland) to quantify the degree of hydrophobicity. For this purpose, a water droplet of 12 μl was placed at each of three different locations on the surface of the hydrophobic aerogel, and the average value was then taken as the contact angle (θ). Microstructural studies of the aerogel samples were performed by transmission electron microscopy (TEM, JSM 6700 F, JEOL Ltd., Japan).

RESULTS AND DISCUSSION

1. Mechanisms of Simultaneous Solvent Exchange and Surface Modification of the Hydrogel

Generally, the silica network that is developed through polymerization of colloidal silica is weak. As the liquid, which coexists with vapor within the pores of the gel, begins to evaporate during the drying process, a meniscus forms at the liquid-vapor interface. This interface generates surface tension, which develops concave menisci in the pores of the gel. With progressive evaporation, the interface meniscus recedes into the gel body and builds compressive force that acts on the walls of the pores. Shrinkage, due to partial collapse of the gel network [38], results. In addition, the terminal silanol groups (Si-OH) present on the silica surface undergo condensation, forming new siloxane bonds that ultimately result in irreversible shrinkage of the gel [39]. This irreversible shrinkage of the gel network can be reduced by attaching alkyl groups to the silica surface by replacing the alkyl group (R) from OH. Additionally, gel collapse ceases when the gel structure is strong enough to withstand the tensile strength of the liquid. Therefore, to reduce irreversible shrinkage of the gel during the drying process, in this study, the surface of the gels was organically modified by tri-methyl groups (found in TMCS) via simultaneous solvent exchange and surface modification using methanol/TMCS/n-hexane solution. The expected chemical reactions for the one-step solvent exchange and surface modification of the gels are:

$$(CH_3)_3Si\text{-}Cl[TMCS]+CH_3OH\rightarrow(CH_3)_3\text{-}Si\text{-}O\text{-}CH_3[MTMS]+HCl \quad (3)$$

$$2(CH_3)_3Si\text{-}Cl[TMCS]+H_2O \rightarrow(CH_3)_3\text{-}Si\text{-}O\text{-}Si\text{-}(CH_3)_3[HMDSO]+2HCl \quad (4)$$

$$2(CH_3)_3\text{-}Si\text{-}O\text{-}CH_3+H_2O\rightarrow(CH_3)_3\text{-}Si\text{-}O\text{-}Si\text{-}(CH_3)_3+2CH_3OH \quad (5)$$

$$(CH_3)_3\text{-}Si\text{-}Cl+\equiv Si\text{-}OH\rightarrow\equiv Si\text{-}O\text{-}Si(CH_3)_3+HCl \quad (6)$$

Thus, TMCS reacts with the methanol (Eq. (3)), pore water (Eq. (4)), and OH groups of the silica surface (Eq. (6)), to form methyltrimethoxysilane [MTMS], hexamethyldisiloxane (HMDSO). Consequently, the hydrophilic surface of the silica network becomes hydrophobic. As the reaction proceeds, transferable liquids (HCl/residual methanol) spontaneously exit the wet gel [40]. During the simultaneous solvent exchange/surface modification process, the reaction between methanol and TMCS can help to reduce the reaction rate of TMCS with OH groups on the silica surface. This process spontaneously replaces pore water with n-hexane, as shown in Fig. 1. The chemical surface modification of the hydrogels by non-polar alkyl/aryl groups is an indispensable step before the APD, prohibiting the formation of new siloxane bonds between the adjacent silica cluster and thereby preventing irreversible shrinkage of the gel [41,42]. In the present work, the surface of the sodium silicate-based hydrogels was organically modified by tri-methyl groups present in trimethylchlorosilane by simultaneous solvent exchange and surface modification process.

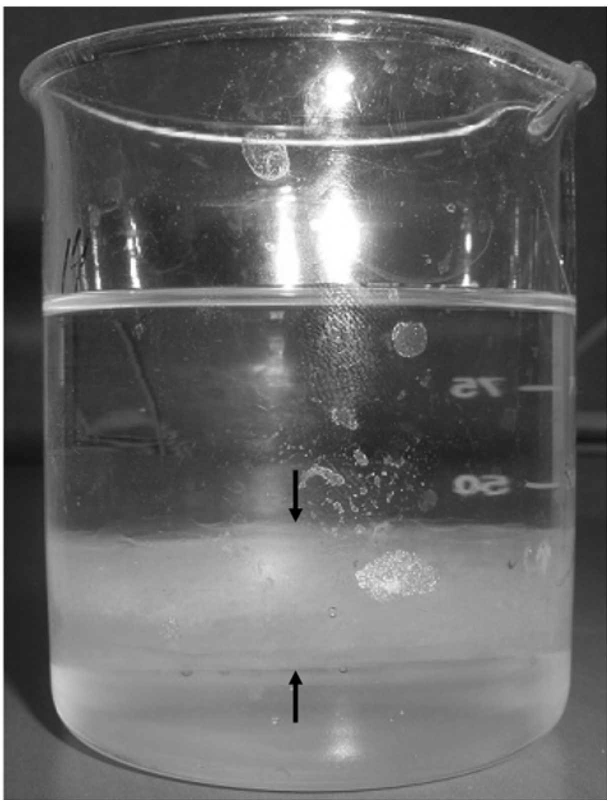

Fig. 1. Floating of the gel while simultaneous chemical surface modification and solvent exchange in n-hexane.

Table 1. The physical properties of aerogels synthesized by different methanol/TMCS molar and n-hexane/TMCS volume ratios

Sr. No	Methanol/TMCS molar ration (M)	n-Hexane/TMCS volume ratio (V)	Remarks
1	0.5	-	Pieces
2	1	-	Pieces
3	1.5	-	Pieces
4	2.0	-	Pieces
5	1	10	Cracks
6	1	15	Cracks
7	1	20	Multiple cracks
8	1	25	Few cracks
9	1	30	Multiple cracks

2. Effect of Methanol/TMCS Molar (M) and n-Hexane/TMCS Volume (V) Ratios on the Physical Properties of Sodium Silicate-based Silica Aerogels

Table 1 shows the physical properties of aerogels synthesized by different methanol/TMCS molar and n-hexane/TMCS volume ratios. The molar ratio of methanol/TMCS was varied from 0.5 to 2, and the volumetric ratio of n-hexane and TMCS was varied from 10 to 30. No significant effect of methanol/TMCS on the monolithicity of the dried aerogels was observed at the experimental molar ratios. As a result, the molar ratio of methanol/TMCS was maintained at 1. However, the volume ratio of n-hexane/TMCS strongly influenced the physical and textural properties of the resulting aerogels. Fewer cracks were observed in aerogels when the volumetric ratio of n-hexane/TMCS was 25, as observed in related studies [33,43]. Therefore, for further experiments, the volumetric ratio of n-hexane/TMCS was fixed at 25.

3. Effect of Aging Time (t) and Temperature (T) on Volume Shrinkage, Bulk Density, and Porosity

Aerogels are brittle due to the high porosity, and enhancement of the mechanical strength of the aerogels is essential to preserve its porosity during ambient pressure drying. In addition to the change in crosslinking density during aging, coarsening and microscopic phase separation may occur and affect the surface and pore structure of a dried gel. In addition, the aging of a gel strengthens the network stiffness without a significant reduction in pore size. The extent of shrinkage that occurs during ambient pressure drying depends on the strength and stiffness of the network [44]. Extending the aging time can increase the framework strength of a silica gel, and increasing the aging temperature can shorten the aging period and, consequently, affect the pore size [25,45].

During the aging process, material is transported to the neck region between particles, producing a more rigid gel network. The driving force for the material transport is the difference in the solubility, s, for surfaces with different curvatures, r, given by the Kelvin Eq. (7):

$$s=s_0\exp\left(\frac{2\gamma_{sl}V_m}{RTr}\right) \quad (7)$$

where s_0 is the solubility of a flat surface of the solid phase, γ_{sl} is the solid-liquid interfacial energy, V_m is the molar volume of the solid, R is the ideal gas constant, and T is the temperature. Necks between particles have a negative curvature (r<0) and, hence, a low solubility. Material accumulates in these convex areas after being transported from the concave surface of a particle. The smaller the particle, the larger the solubility, such that the driving force also acts to dissolve the smallest particles, followed by precipitation onto larger particles. However, this ripening mechanism leads to a coarsening of the structure and occurs after too long an aging time [25]. The coarsening mechanism, in which the particles dissolve and reprecipitate onto larger particles, also leads to an increase in pore size. The capillary pressure decreases according to Eq. (8):

$$\mathrm{Pr} = \frac{-2\gamma\cos\theta}{\mathrm{R}} \tag{8}$$

where, γ is the surface tension of the liquid, θ is the contact angle between the walls of the pore and liquid, R is the radius of the pore, and Pr is the capillary pressure which causes stress in the gel during drying. An increase in pore size, which decreases capillary pressure and, hence, drying stress in the gel network, therefore reduces linear drying shrinkage. Hence, low-density monolithic silica aerogels can be obtained as a result of the increase in stiffness and pore size of the gel, which reduces the shrinkage during drying. Aging conditions (temperature and time) have a strong impact on the physical properties of the silica aerogels: volume shrinkage, bulk density, porosity, monolithicity, and contact angle.

Effects of the gel aging temperature and time on the volume shrinkage (%), density, and porosity (%) were studied by varying the aging temperature and time from ~25 to 80 °C (Table 1) and 6 to 24 hrs, respectively. Fig. 2 shows the effect of aging time (t) with respect to temperature (T) on the volume shrinkage of the aerogels. The percentage of volume shrinkage decreased with an increase in aging time up to 18 hours. Further increase in aging time up to 24 hours caused more volume shrinkage, resulting in an increase in bulk density. However, at higher gel aging temperatures (80 °C), the volume shrinkage increased continuously with increasing aging time from 6 to 24 hour. The variation in bulk density with temperature with respect to gel aging time is depicted in Fig. 3. As shown there, the lowest dense silica aerogel was obtained at an aging temperature of 60 °C for 18 hours. It was previously reported that the condensation of surface -OH groups, syneresis, coarsening, and segregation (which occur during aging) strongly affect the properties of dried silica aerogels [46].

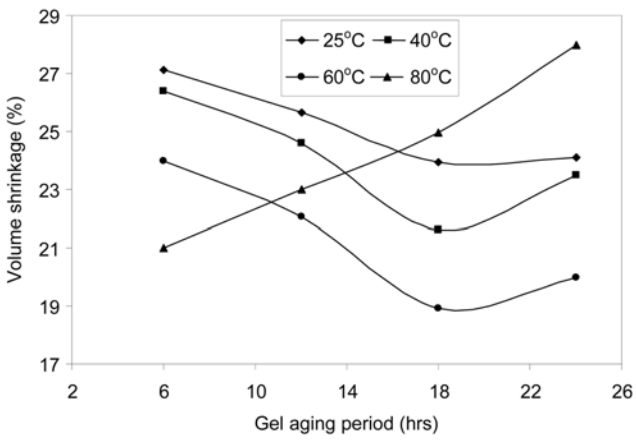

Fig. 2. Effect of gel aging time and temperature on the volume shrinkage (%).

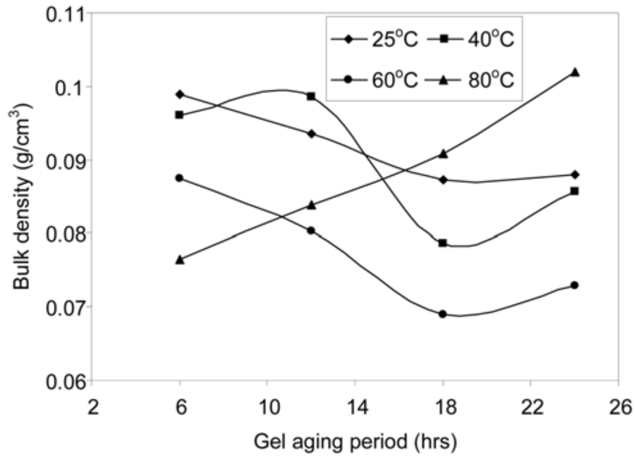

Fig. 3. Effect of gel aging time and temperature on the bulk density.

The lowest bulk density in the present study was observed at the aging temperature of 60 °C for 18 hours. This result indicates that, at this aging condition, the dissolution and reprecipitation of silica particles occur more strongly, consequently depositing at the negative radius of the curvature, causing the neck growth between the particles, and leading to increasing characteristic pore size. As a result, the capillary pressure was lower (as demonstrated using Eqs. (7) and (8)), and the aerogels were probably stiffer and stronger. In the latter case, a low-density, silica aerogel was obtained due to less shrinkage during APD. Fig. 4 shows the variations in the porosity percentage in relation to the aging temperature and time. Evidently, the porosity percentage increases with aging temperature. Additionally, the porosity percentage increases with an aging time up to 18 hours, although further increase in aging time decreases the porosity. This finding is attributable to an increase in aging temperature leading to more shrinking of the gel, which leads to an increase in the volume shrinkage and the bulk density of the aerogels. Hence, the porosity percentage increases with aging temperature accord-

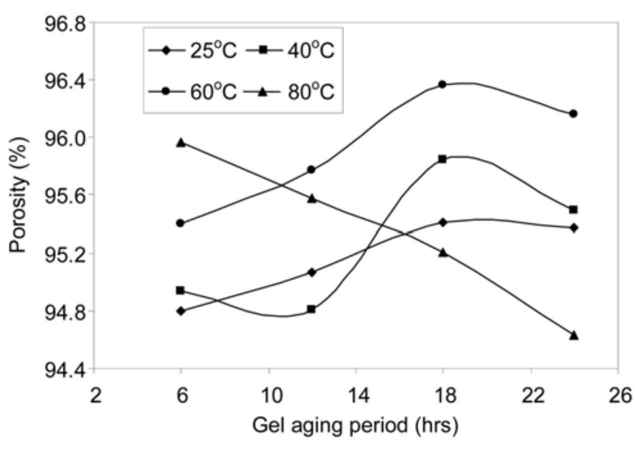

Fig. 4. Effect of gel aging time and temperature on the porosity (%).

Table 2. Effect of aging temperature on the physical and textural properties of the sodium silicate-based silica aerogels prepared by simultaneous solvent exchange surface modification followed by ambient pressure drying

Sr. No	Aging time (hrs)	BET surface area (m^2/g)	Pore size (nm)	Pore volume (cm^3/g)	Remarks
		Aging temperature 25 °C			
1	0 (unaged)	829	7.8	3.56	Pieces
2	6	833	8.2	3.41	Pieces
3	12	836	8.5	2.31	Cracks
4	18	840	9.8	3.20	Few cracks
5	24	847	10.3	3.15	Monolithic
		Aging temperature 40 °C			
1	6	841	11.4	3.38	Cracks
2	12	835	12.6	3.46	Few cracks
3	18	829	13.4	3.50	Few cracks
4	24	819	13.9	3.61	Monolithic
		Aging temperature 60 °C			
1	6	834	13.5	3.39	Cracks
2	12	827	14.8	3.52	Few cracks
3	18	820	15.4	3.80	Monolithic
4	24	811	16.1	3.86	Few cracks
		Aging temperature 80 °C			
1	6	807	14.5	3.48	Few cracks
2	12	792	16.2	3.62	Few cracks
3	18	785	17.4	3.83	Cracks
4	24	764	18.6	3.91	Cracks

ing to Eq. (2). Therefore, the capillary pressure decreases with the increase in pore size, resulting in a decrease in linear volume shrinkage. Reduction in porosity percentages with more than 18 hours aging may be associated with the extensive shrinkage that occurs during prolonged gel aging.

4. Effect of Aging Time (t) and Temperature (T) on Monolithicity

Aging a gel before APD helps to strengthen the silica network, reducing the risk of fracture during drying [46]. As mentioned in Table 2, at lower aging times and higher aging temperatures, the probability of fracturing the silica network is high during the drying process. Specifically, with less aging, the silica network was not stiff or strong enough to prevent cracks. Moreover, a few cracks were observed in the aerogel that was dried above 60 °C, whereas, absolutely monolithic silica aerogels were obtained at an aging temperature of 60 °C for 18 hours, attributable to the higher aging temperature of the gel strengthening the gel network. Higher aging temperature also increases the pore size and considerably reduces the capillary pressure [30]. Thus, a gel that can withstand the drying stress can develop into a monolithic silica aerogel.

5. Effect of Aging Temperature (T) on Hydrophobic Properties

To determine the effect of aging temperature on the hydrophobic properties of sodium silicate-based silica aerogels, the aging temperature before surface modification of the gel was varied from room temperature to 80 °C, while the aging period was maintained at 18 hrs. The effect of the aging temperature on the hydrophobic properties of silica aerogels was studied by measuring the water contact angle on the silica aerogel surface. The observed hydrophobicity was attributed to the attachment of hydrolytically stable -Si-$(CH_3)_3$ groups after replacement by CH_3 of the -OH groups on the silica surface. A slight increase in the contact angle of the aerogels occurred at some aging temperatures. The contact angle was greatest (160°) for the aerogels aged at 60 °C for 18 hours (Fig. 5). As shown in Fig. 6, the hydrophobicity of the silica aerogel was tested by placing the silica aerogel directly on the water surface.

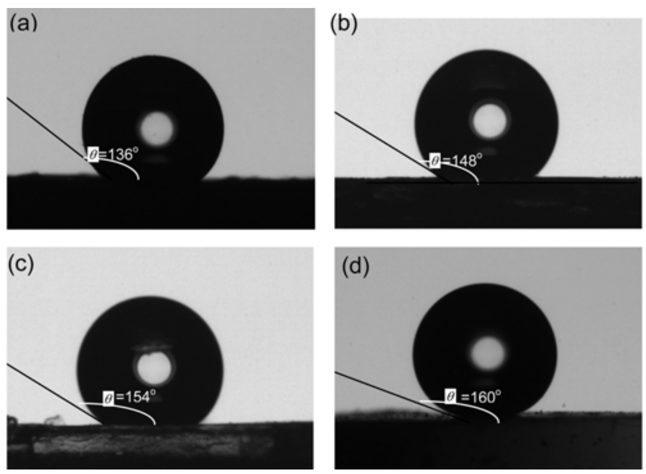

Fig. 5. Water droplets placed on the hydrophobic silica aerogels surfaces prepared with different aging temperature of the gel at fixed aging time (18 hr) (a)25 °C (b) 40 °C (c) 60 °C and (d) 80 °C.

Surface modification of the gels was also confirmed by Fourier transform infrared (FTIR) spectroscopy, as shown in Fig. 7. Besides the Si-O-Si absorption peak at 1,060 cm^{-1}, all aerogel samples showed Si-CH_3 peaks at 850 and 1,260 cm^{-1} [30,47,48]. The presence of

Fig. 6. The monolithic hydrophobic silica aerogel floating on the surface of water.

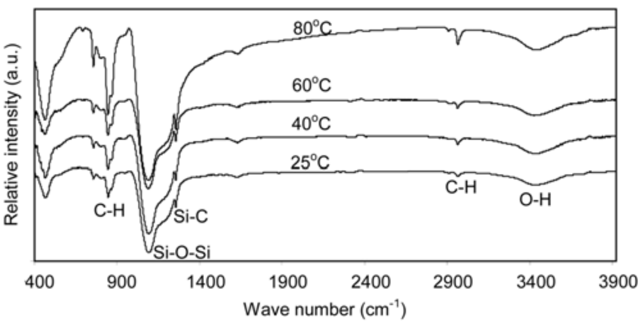

Fig. 7. FTIR spectra of the TMCS modified sodium silicate-based silica aerogels prepared with different aging temperature of the gel at fixed aging time (18 hr).

Si-CH_3 peaks in the FTIR spectra of all the aerogel samples confirms the successful attachment of -SiCH_3 groups from the TMCS to the silica aerogel surface upon surface modification of the aerogels. The degree of intensity of the Si-CH_3 peaks depends on the aging temperature. The intensity of the O-H band decreased, while that of the Si-C and C-H bands increased with aging temperatures from ~25 to 80 °C, due to the increase in Si$(CH_3)_3$ groups attached to the silica gel surface. Better surface modification of the gel occurred at higher aging temperatures. Due to the surface modification process, the aerogels exhibited hydrophobic behavior.

To investigate the thermal stability or the hydrophobic nature of the silica aerogels, samples were heated in a furnace at various temperatures. The aerogels retained their hydrophobic behavior up to 520 °C, above which they became hydrophilic. At this temperature, the surface methyl groups (-CH_3) are oxidized, resulting in the formation of a hydrophilic aerogel. In addition, the thermal stability of the aerogels and oxidation temperature for the -CH_3 groups were estimated by thermogravimetric (TG) and differential thermal (DT) analyses, respectively. Fig. 8 shows the TG-DT analysis of the aerogels aged at 60 °C for 18 hours in an oxygen atmosphere up to 1,000 °C. The TG-DTA curves clearly show that the aerogels aged at 60 °C and modified with TMCS exhibited a negligible weight loss up to a temperature of 520 °C, beyond which the aerogel underwent significant weight loss. This decrease in weight is due to the oxidation of the surface methyl groups confirmed by the sharp exothermic peaks in the DTA curve when the temperature was above 520 °C [49].

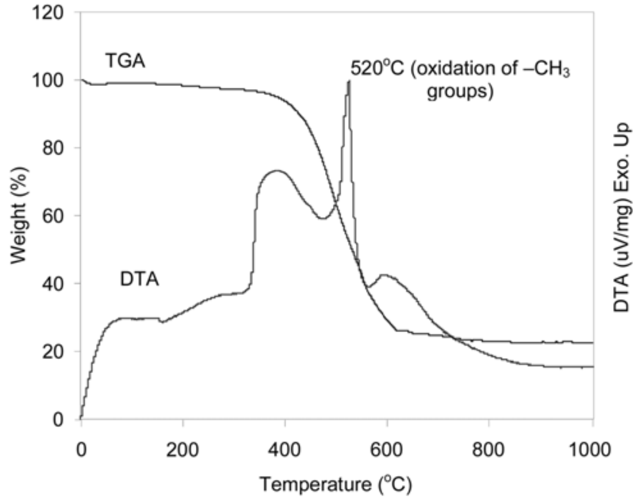

Fig. 8. TG-DTA curve of an ambient pressure dried sodium silicate-based hydrophobic silica aerogel.

6. The Combined Effect of Aging Time and Temperature on the Textural Properties

The effect of aging time and temperature on the textural properties of silica aerogels were investigated by varying the aging time from 6 to 24 hrs and the aging temperature from room temperature (~25 °C) to 80 °C. To obtain the effect of aging time on the textural properties of silica aerogels, the aging time was varied from 0 to 24 hrs while maintaining the temperature at ~25 °C (room temperature). Further, to observe the effect of the aging temperature on the textural properties of silica aerogels, the aging temperature was varied from 25 to 80 °C, and the aging time was fixed at 18 hours. The effects of the aging time and temperature on the specific surface area, pore volume, and pore size were determined by the standard BET and BJH methods, as summarized in Table 2. All aerogels exhibited specific surface areas in the range of 750 to 850 m^2g^{-1}. There was a slight increase in the surface area, pore volume, and pore size with increasing aging time (aging at room temperature). Alternatively, significant changes were observed for the specific surface area, pore volume, and pore size of the aerogels aged at a higher temperature (>25 °C). The specific surface area decreased with increasing gel aging time (0 to 24 hrs) and temperature (>25 °C). However, the cumulative pore volume and pore size increased with increasing gel aging time and temperature. The average pore diameter (P_d) of the aerogels aged at room temperature ranged from 7.8 to 10.3 nm while the aging period varied from 0 to 24 hrs. Alternatively, the average pore diameter obtained for the aerogels aged at a fixed aging period (18 hrs) ranged from 9.8 to 17.4 nm while the

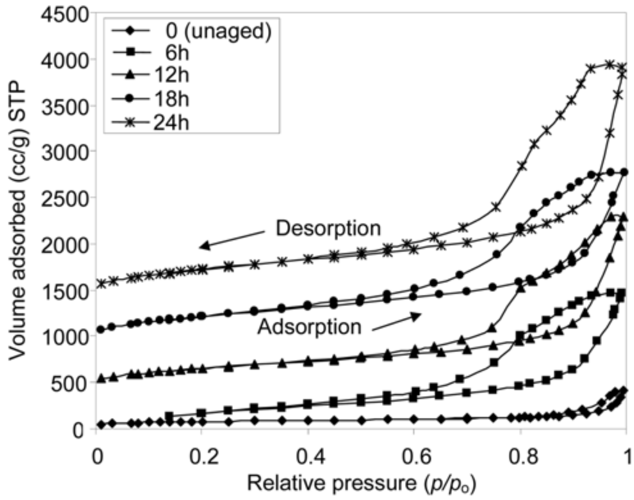

Fig. 9. Effect of aging period of the gel on the N_2 adsorption-desorption isotherms.

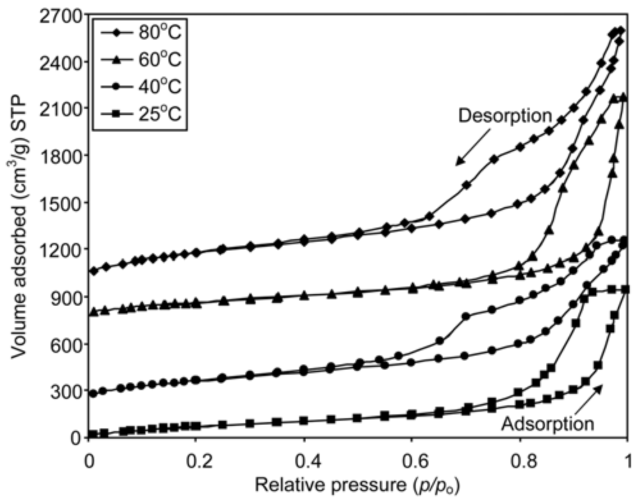

Fig. 10. Effect of aging temperature of the gel on the N_2 adsorption-desorption isotherms.

aging temperature varied from ~25 to 80 °C. The capillary pressure can be reduced by a larger pore size when the gel is dried at ambient pressure. As a result, the aerogel underwent less shrinkage and developed a high pore volume [41,50-52]. Thus, the aging time and temperature influenced the porosity of the final product.

The porosity properties of aerogels obtained at different aging times and temperatures were further compared by examining the nitrogen adsorption-desorption isotherms and pore size distributions. Figs. 9 and 10 show the nitrogen adsorption and desorption graphs for aerogels obtained at different aging conditions. The maximum amount of N_2 gas absorbed for aerogel samples aged at low temperature (~25 °C) was less than for samples aged at higher temperatures (above room temperature). This finding is due to gels aged at a lower temperature having small-sized pores, whereas those aged at higher temperatures having large-size pores. Thus, the increase in aging temperature resulted in the increase in pore size that caused an increase in pore volume. The physisorption isotherms obtained for all the aerogels exhibited hysteresis loops, which corresponded

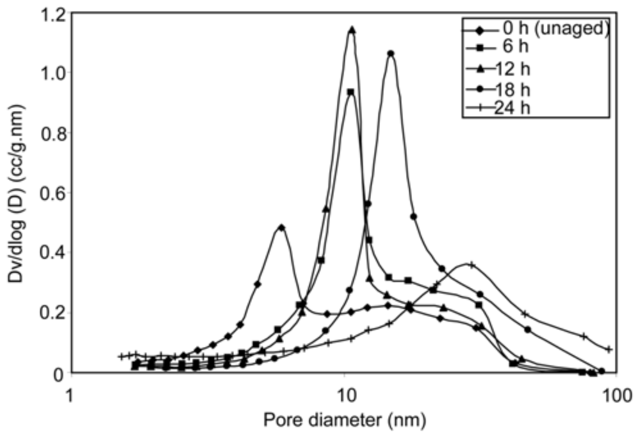

Fig. 11. Effect of aging period of the gel on the BET pore size distribution profiles.

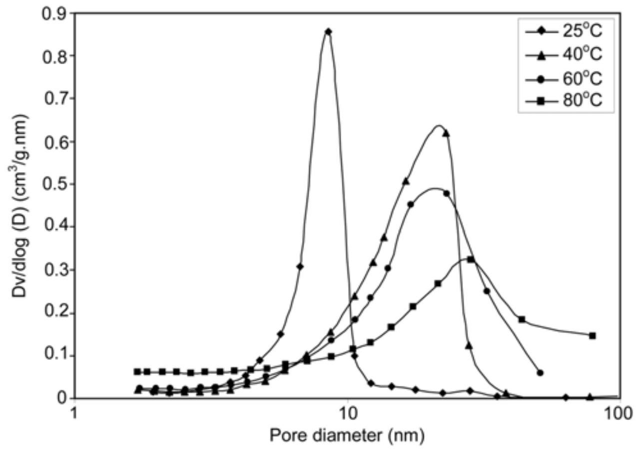

Fig. 12. Effect of aging temperature of the gel on the BET pore size distribution profiles.

to the characteristic feature of the mesoporous materials (Type IV isotherms) [53,54].

Figs. 11 and 12 show the pore size distribution (PSDs) profiles of the silica aerogels obtained at different aging conditions. A significant change was observed in the PSDs profiles of the aerogels obtained at different temperatures. A slight change was observed in the PSDs profile of the aerogels aged at lower temperatures. As shown in Fig. 12, the peak pore diameter shifted to a larger size as the aging temperature increased from ~25 to 80 °C. In contrast, the PSD profiles for the aerogels aged at higher temperatures had a higher-diameter scale (>11 nm) with broad distribution. The aerogels aged with a lower temperature had a narrow PSD at 10 nm, indicating uniform pore distribution throughout the gel network. According to the IUPAC classification of the pores [55], all aerogel samples aged under different conditions showed a pronounced peak in the mesopore region (20-500 Å). This is a characteristic feature of mesoporous materials, indicating that the aerogels developed in the present study maintain mesoporosity in their structure even after drying.

To observe the effect of the aging temperature on the nanostructure of the aerogels, a considerable investigation was performed using transmission electron microscopy (Fig. 13). As previously

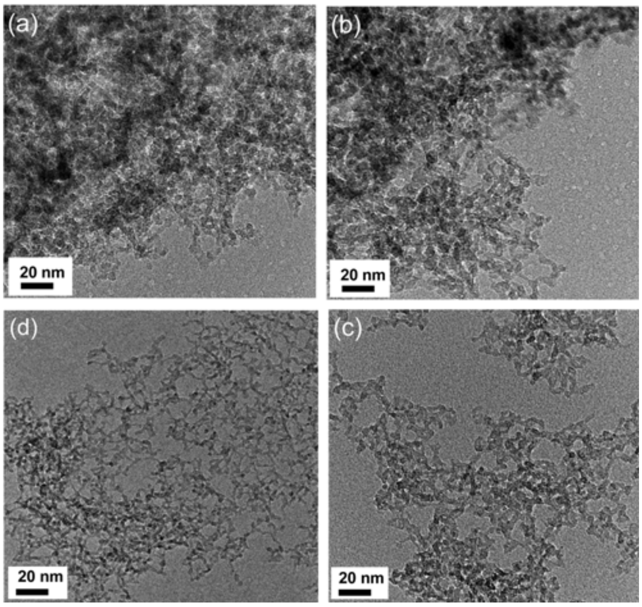

Fig. 13. TEM micrographs of the sodium silicate-based silica aerogels prepared at various aging temperature of the gel at fixed aging time (18 hr) (a) 25 °C (b) 40 °C (c) 60 °C and (d) 80 °C.

demonstrated (the PSD profiles for the samples aged at higher temperature), the aerogels were comprised of large pores of uniform size in the gel network. This observation was empirically supported by the TEM micrographs presented in Fig. 13. Specifically, as the aging temperature of the gel increased, the pore size also increased. In addition, the aerogels synthesized by aging the wet gel at 60 °C showed a well-developed nano-porous structure consisting of aggregates of primary particles that were ~4 nm in size, as shown in Fig. 13(c).

CONCLUSIONS

The optimum conditions for gel aging before surface modification for the synthesis of sodium silicate-based monolithic silica aerogels at ambient pressure are reported. The resulting silica aerogels possessed low bulk density and high porosity, similar to those produced by conventional supercritical drying. This approach is successful because gel aging at the optimum temperature reduces the aging period that is necessary for the synthesis of monolithic silica aerogels at ambient pressure. A sufficient chemical modification can be achieved by simultaneous solvent exchange and surface modification treatment with methanol/TMCS/n-hexane. Monolithic sodium silicate-based silica aerogels with extremely low density (0.069 g/cm^3) and large surface area (820 m^2/g) were synthesized by aging the gel at 60 °C for 18 hours through simultaneous surface modification and drying processes at ambient pressure. The new method suggested in this study is an essential and easy way to synthesize sodium silicate-based (low-cost) monolithic silica aerogels with desired properties at ambient pressure.

ACKNOWLEDGEMENT

We would like to thank the Ministry of Commerce and Industries of the Republic of Korea for financial support under the R & D Innovation Fund for Small and Medium Business Administration (Project Application No. S1017370).

REFERENCES

1. L. W. Hrubesh, *Chem. Ind*., **17**, 824 (1990).
2. G. C. Bond and S. Flamerz, *Appl. Catal*., **33**, 219 (1987).
3. A. V. Rao and R. R. Kalesh, *Sci. Technol. Adv. Mater*., **4**, 509 (2003).
4. K. Kim, K. Y. Jang and R. S. Upadhey, *J. Amer. Ceram. Soc*., **78**, 1997 (1991).
5. G. M. Pajonk, *Appl. Catal*., **72**, 217 (1991).
6. Y. K. Akimov, *Instruments and Experimental Techniques*, **46**, 287 (2003).
7. G. M. Pajonk and S. J. Tichner, in: J. Fricke (Ed.), Processings of the First International symposium on Aerogels, Wurzburg, Germany, 23-25, September 193 (1985).
8. S. T. Reed, C. S. Ashley, C. J. Brinker, R. J. Walko, R. Ellefsoon and J. Gill, *SPIE*, **1328**, 220 (1990).
9. J. P. Cunha, F. Neves and M. I. Lopes, *Nucl. Instrum. Methods Phys. Res. A*, **452**, 401 (2001).
10. C. J. Brinker and S. W. Sherere, *Sol-Gel Sci*., Academic Press, San Diego, 501 (1990).
11. T. Sumiyoshi, I. Adachi, R. Enomoto, T. Iijima, R. Suda, M. Yokoyama and H. Yokogawa, *J. Non-Cryst. Solids*, **225**, 369 (1998).
12. M. Schmidt and F. Schwertfeger, *J. Non-Cryst. Solids*, **225**, 364 (1998).
13. L. W. Hrubesh, *J. Non-Cryst. Solids*, **225**, 335 (1998).
14. J. E. Fesmire, *Cryogenics*, **46**, 111 (2006).
15. T. J. Yim, S. Y. Kim and K. P. Yoo, *Korean J. Chem. Eng*., **19**(1), 159 (2002).
16. T. M. Harris, V. D. Land and D. C. Teeters, *J. Non-Cryst. Solids*, **283**, 11 (2001).
17. C. J. Lee, G. S. Kim and S. H. Hyun, *J. Sol-Gel Sci. Technol*., **37**, 2237 (2002).
18. F. Shi, L. Wang and J. Liu, *Mater. Lett.*, **60**, 29 (2006).
19. H. J. Hwang, C. E. Kim and J. S. Yoon, *J. Sol-Gel Sci. Technol*., **49**, 47 (2009).
20. A. V. Rao, A. P. Rao, P. M. Shewale and S. D. Bhagat, *J. Sol-Gel Sci. Technol*., **49**, 285 (2009).
21. F. Schwertfeger, D. Frank and M. Schmidt, *J. Non-Cryst. Solids*, 225, 24 (1998).
22. D. M. Smith, D. Stein, J. M. Anderson and W. Ackerman, *J. Non-Cryst. Solids*, **186**, 104 (1995).
23. S. K. Kang and S. Y. Choi, *J. Mater. Sci*., **35**, 4971 (2000).
24. H. H. Jung, S. W. Hwang, S. H. Hyun and Y. S. Ahn, *J. Sol-Gel Sci. Tech*., **41**, 139 (2007).
25. S. Hæreid, J. Anderson, M. A. Einarsrud, D. W. Hua and D. M. Smith, *J.Non-Cryst. Solids*, **185**, 221 (1995).
26. G. Reichenauer, *J.Non-Cryst. Solids*, **350**, 189 (2004).
27. D. J. Suh, T. J. Park, J. H. Sonn, H. Y. Han and J. C. Lim, *Korean J. Chem. Eng.*, **17**(1), 101 (2000).
28. Fang He, H. Zhao, X. Qu, C. Zhang and W. Qiu, *J. Mater. Process. Tech*., **209**, 1621 (2009).
29. A. B. Jarzebski, J. Lorenc, Y. I. Aristov and N. Lisitza, *J. Non-Cryst. Solids*, **190**, 198 (1995).
30. R. Takahasi, K. Nakanishi and N. Soga, *J. Non-Cryst. Solids*, **189**,

66 (1995).
31. Z.-J. Li, C.-R. Liu and Q.-S. Zhao, *J. Non-Cryst. Solids*, **265**, 189 (2000).
32. P. M. Shewale, A. V. Rao, A. P. Rao and S. D. Bhagat, *J. Sol-Gel Sci. Technol*., **49**, 285 (2009).
33. S. W. Hwang, T. Y. Kim and S. H. Hyunm, *J. Colloid Interf. Sci*., **322**, 224 (2008).
34. C. J. Brinker and S. W. Sherere, *Sol-Gel Sci*., Academic Press, San Diego, 662 (1990).
35. R. Rouquerol, D. Avnir, C. W. Fairbridge, D. H. Everett, J. H. Haynes, N. Pernicone, J. D. F. Ramsay, K. S. W. Sing and K. K. Unger, *Pure Appl. Chem.*, **66**, 1739 (1994).
36. F. Rouquerol and K. S. W. Sing, *Jean rouquerol - adsorption by powders and porous solids: Principles*, Methodology and Applications, Academic Press (1998).
37. Z. Bi, Z. Zhang, F. Xu, Y. Qian and J. Yu, *J. Colloid Interf. Sci*., **214**, 368 (1999).
38. H. D. Gesser and P. C. Goswami, *Chem. Rev.*, **89**, 765 (1989).
39. S. D. Bhagat, Y. H. Kim, G. B. Yi, Y. S. Ahn and J. G. Yeo, *Microporous and Mesoporous Materials*, **253**, 3231 (2006).
40. L. J. Wang, S. Y. Zhao and M. Yang, *Mater. Chem. Physics*., **113**, 485 (2009).
41. R. Deshpande, D. M. Smith and C. J. Brinker, *J. Non-Cryst. Solids*, **144**, 32 (1992).
42. X. C. Zhou, L. P. Zhong and Y. P. Xu, *Inorganic Mater.*, **44**, 976 (2008).
43. M. Laczka, K. C. Kowalska and M. Kogul, *J. Non-Cryst. Solids*, **287**, 10 (2007).
44. C. J. Brinker and G. W. Scherer, *J. Non-Cryst. Solids*, **70**, 301 (1985).
45. S. Smitha, P. Shajesh, P. R. Aravind, S. Rajesh Kumar, P. Krishna Pillai and K. G. K. Warrier, *Microporous and Mesoporous Materials*, **91**, 286 (2006).
46. Uzma K H Bangi, A. V. Rao and A. P. Rao, *Sci. Technol. Adv. Mater*., **9**, 35006 (2008).
47. H. E. Rassy and A. C. Pierre, *J. Non-Cryst. Solids*, **351**, 1603 (2005).
48. A. Y. Jeong, S. M. Goo and D. P. Kim, *J. Sol-Gel Technol*., **19**, 483 (2000).
49. A. P. Rao, A. V. Rao, G. M. Pajonk and P. M. Shewale, *J. Mater. Sci*., **42**, 8418 (2007).
50. G. W. Scherer, S. Haereid, E. Nilsen and M. A. Einarsud, *J. Non-Cryst. Solids*, **202**, 104 (1996).
51. A. P. Rao, A. V. Rao and J. L. Gurav, *J. Porous Mater*., **15**, 507 (2008).
52. A. P. Rao, A. V. Rao and G. M. Pajonk, *Appl. Surf. Sci*., **253**, 6032 (2007).
53. A. C. Pierre, E. Elaloui and G. M. Pajonk, *Langmuir*, **14**, 66 (1998).
54. W. C. Li, A. H. Lu and S. C. Guo, *J. Colloid Interf. Sci*., **254**, 153 (2002).
55. K. S. W. Sing, D. H. Everett, R. A. W. Haul, L. Moscou, R. A. Pierotti, J. Rouquerol and T. Siemieniewska, *Pure Appl. Chem*., **57**(4), 603 (1985).